

Electronic Supplementary Information

Label-free Optical Bio-Sensing of Non-cancerous and Cancerous Tissues from Mice: Distinct Spectroscopic Features of Thiazole Orange

Ravisha Gala,^{a,†,#} Vishwa V. Gandhi,^{a,b,†} Nilotpal Barooah,^a Amit Kunwar,^{*a,b} Achikanath C. Bhasikuttan,^{*a,b} and Jyotirmayee Mohanty^{*a,b}

^aRadiation & Photochemistry Division, Bhabha Atomic Research Centre, Mumbai, 400085 INDIA. ^bHomi Bhabha National Institute, Training School Complex, Anushaktinagar, Mumbai, 400094, India. [†] Equal Contribution.

[#] Student of Sunandan Divatia School of Science, NMIMS, Mumbai, India.

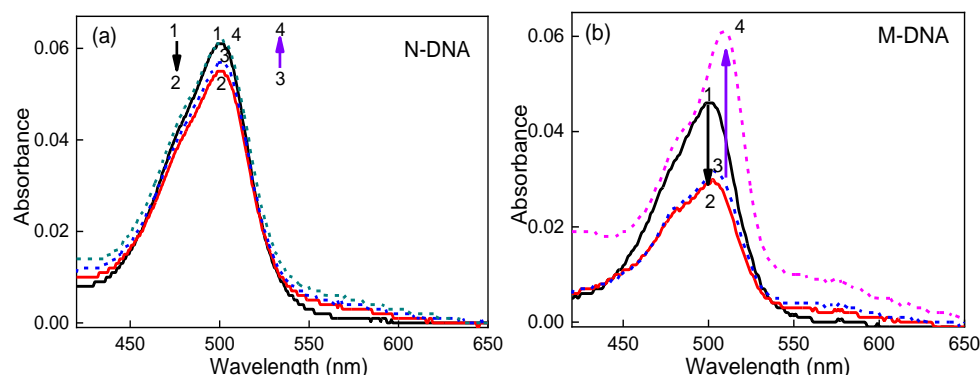


Fig. S1 Absorption spectra of TO ($\sim 4 \mu\text{M}$) at different concentrations of **(A)** [N-DNA]/ μM : (1) 0, (2) 1, (3) 2 and (4) 6. **(B)** [M-DNA]/ μM : (1) 0, (2) 0.4, (3) 0.8 and (4) 29. The above data set is the representative of the individual mouse of C57BL/6J strain.

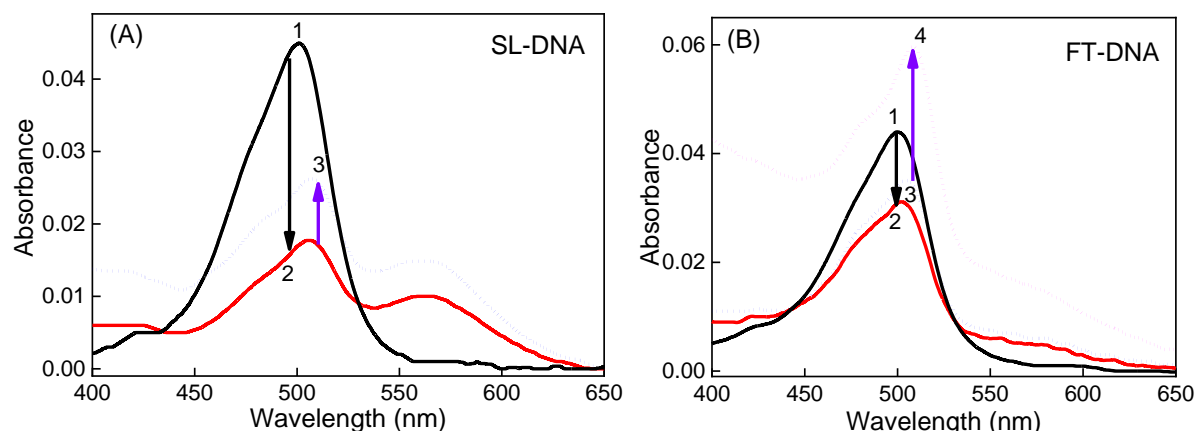


Fig. S2 Absorption spectra of TO ($\sim 4 \mu\text{M}$) at different concentrations of **(A)** [SL-DNA]/ μM : (1) 0, (2) 1, (3) 6; **(B)** [FT-DNA]/ μM : (1) 0, (2) 0.8, (3) 3, (4) 38; The above data set is the representative of the individual mouse of Swiss albino strain.

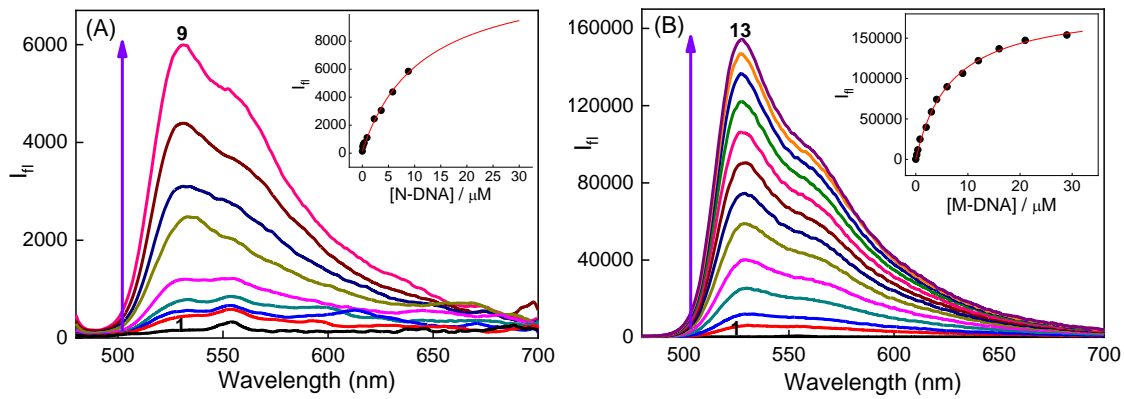


Fig. S3 Steady-state fluorescence spectra of TO (~4 μM) at different concentrations of **(a)** [N-DNA]/ μM : (1) 0, (2) 0.1, (3) 0.2, (4) 0.4, (5) 1, (6) 2, (7) 4, (8) 6, (9) 9. **(b)** [M-DNA]/ μM : (1) 0, (2) 0.2, (3) 0.4, (4) 0.8, (5) 2, (6) 3, (7) 4, (8) 6, (9) 9, (10) 12, (11) 16, (12) 21, (13) 29. **Inset**s show the binding isotherm of TO with the respective DNA. The above data set is the representative of the individual mouse of C57BL/6J strain.

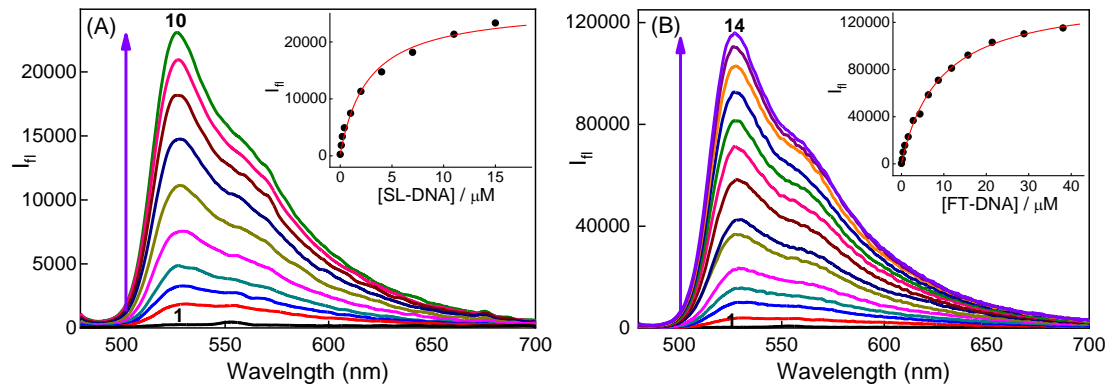


Fig. S4 Steady-state fluorescence spectra of TO (~4 μM) at different concentrations of **(a)** [SL-DNA]/ μM : (1) 0, (2) 0.1, (3) 0.2, (4) 0.4, (5) 1, (6) 2, (7) 4, (8) 7, (9) 11, (10) 15; **(b)** [FT-DNA]/ μM : (1) 0, (2) 0.2, (3) 0.4, (4) 0.8, (5) 2, (6) 3, (7) 4, (8) 6, (9) 9, (10) 12, (11) 16, (12) 21, (13) 29, (14) 38; **Inset**s show the binding isotherm of TO with the respective DNA. The above data set is the representative of the individual mouse of Swiss albino strain.

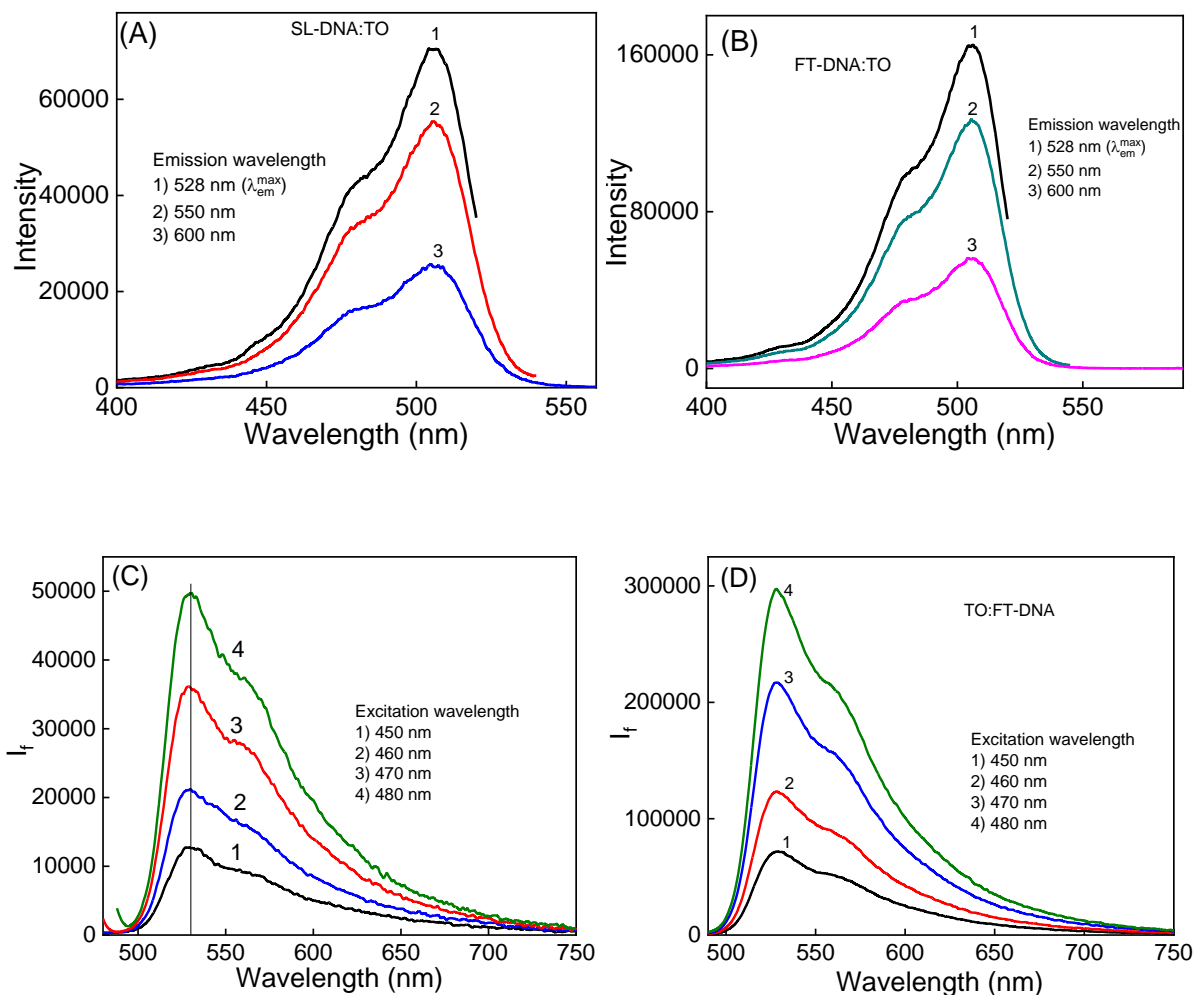


Fig. S5 Excitation spectra of SL-DNA:TO (A) and FT-DNA:TO (B) recorded by choosing three different emission wavelengths. Emission spectra of SL-DNA:TO (C) and FT-DNA:TO (D) recorded by varying excitation wavelengths

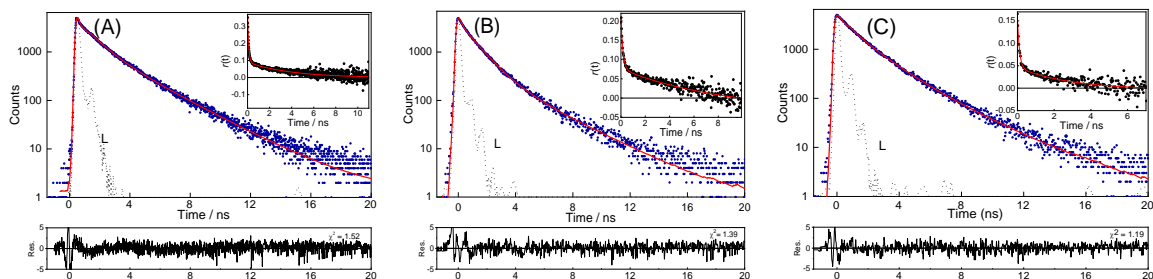
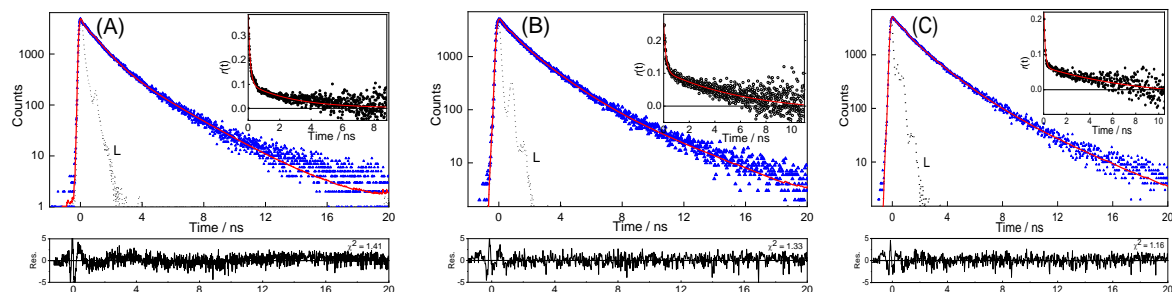
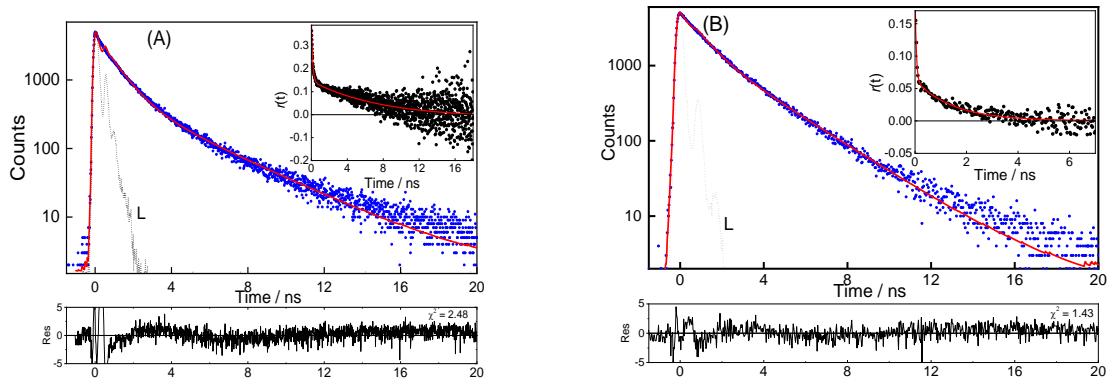


Table S1. Fluorescence lifetime of TO at different concentrations of normal and tumor DNAs.

| Origin of DNA | [DNA] / μM | $\tau_1(\text{ns})$ | a_1 | $\tau_2(\text{ns})$ | a_2 | $\tau_3(\text{ns})$ | a_3 | $\langle \tau \rangle (\text{ns})$ | χ^2 ^{\$} |
|-----------------|-----------------------|---------------------|-------|---------------------|-------|---------------------|-------|------------------------------------|------------------------|
| N-DNA (Normal) | 9.0 | 0.04 [#] | 0.18 | 0.86 | 0.46 | 3.3 | 0.36 | 1.59 | 2.48 ^{\$} |
| M-DNA (Tumor) | 29.0 | 0.04 [#] | 0.06 | 0.81 | 0.36 | 2.46 | 0.58 | 1.72 | 1.43 |
| BL-DNA (Normal) | 9.0 | 0.04 [#] | 0.13 | 0.87 | 0.49 | 2.51 | 0.38 | 1.39 | 1.41 |
| WT-DNA (Tumor) | 29.0 | 0.43 | 0.19 | 1.62 | 0.62 | 3.83 | 0.19 | 1.81 | 1.33 |
| WL-DNA (Tumor) | 29.0 | 1.68 | 0.61 | 1.68 | 0.61 | 3.78 | 0.21 | 1.87 | 1.16 |
| SL-DNA (Normal) | 15.0 | 0.04 [#] | 0.13 | 1.0 | 0.42 | 2.53 | 0.45 | 1.56 | 1.52 |
| FT-DNA (Tumor) | 38.0 | 0.42 | 0.19 | 1.55 | 0.57 | 3.19 | 0.25 | 1.76 | 1.39 |
| FL-DNA (Tumor) | 17.5 | 0.35 | 0.15 | 1.46 | 0.62 | 3.48 | 0.23 | 1.76 | 1.19 |

[#] Considering the limitation of the time resolution, this faster component was fixed the value 40 ps.

^{\$} The increased χ^2 value is due to a fluctuation in the prompt profile and also due to a contribution from scattering developed during the DNA titration.

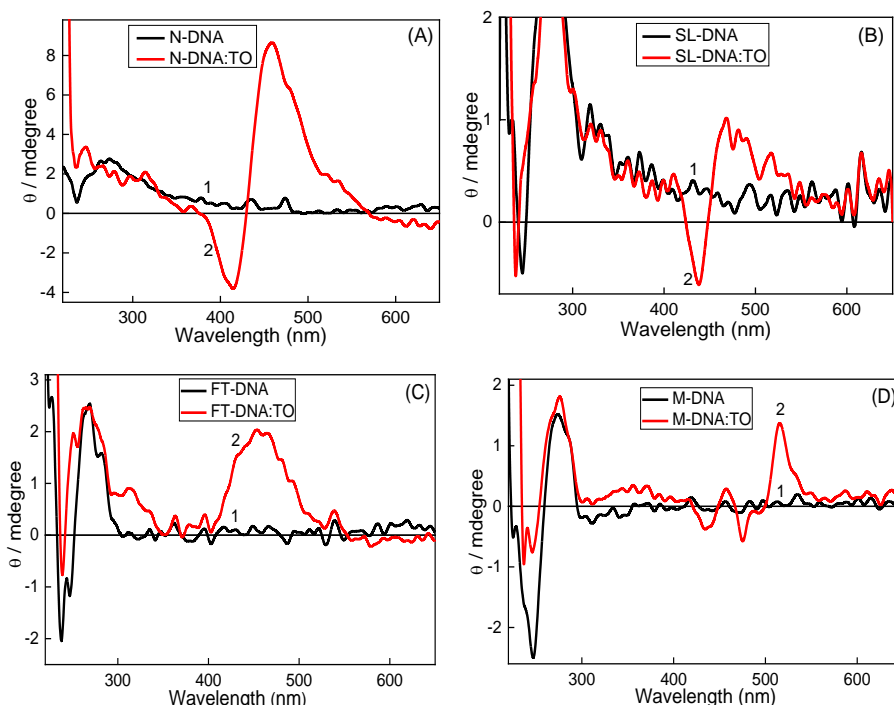


Fig. S9 Circular Dichroism spectra of **(A)** (1) N-DNA (200 μM), (2) N-DNA (200 μM):TO (100 μM), **(B)** (1) SL-DNA (200 μM), (2) SL-DNA (200 μM):TO (100 μM); **(C)** (1) FT-DNA (200 μM), (2) FT-DNA (200 μM):TO (100 μM), **(D)** (1) M-DNA (200 μM), (2) M-DNA (200 μM):TO (100 μM); The above data set is the representative of the individual mouse of C57BL/6J and Swiss albino strain.

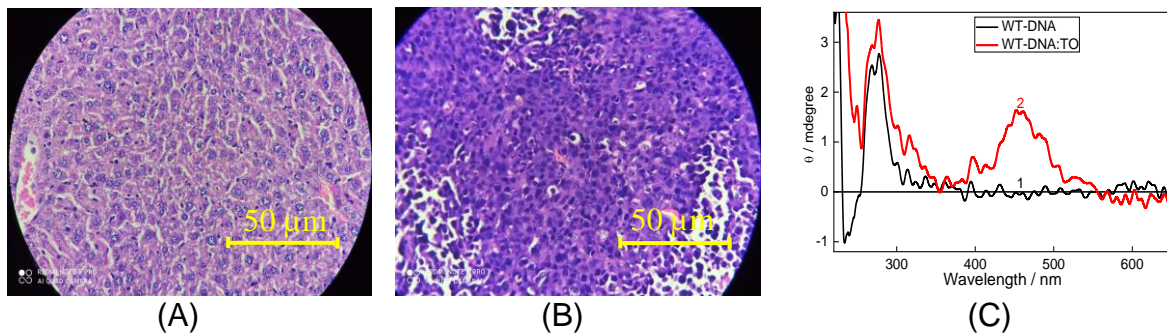


Fig. S10 Representative images of H&E stained tissue section of non-cancerous liver (A) and fibrosarcoma (B) tissues of BALB/c mice. (C) is the CD spectrum recorded from corresponding cancerous DNA-TO complex.

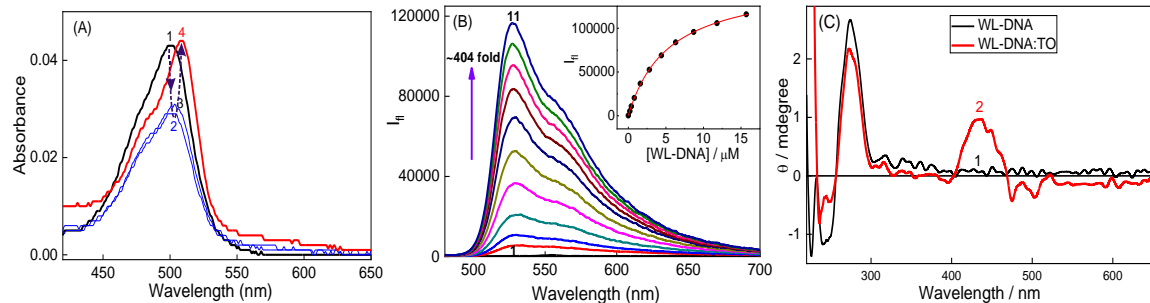


Fig. S11 (A) Absorption of TO with $[WL\text{-DNA}] / \mu\text{M}$: (1) 0, (2) 0.4, (3) 0.8 and (4) 16.; (B) Fluorescence of TO with $[WL\text{-DNA}] / \mu\text{M}$, (1) 0, (2) 0.2, (3) 0.4, (4) 0.8, (5) 2, (6) 3, (7) 4, (8) 6, (9) 9, (10) 12 and (11) 16; (C) CD spectra of TO with (1) WL-DNA (200 μM), (2) WL-DNA (200 μM):TO (100 μM). Inset in (B) shows the binding isotherm of TO with the WL-DNA. The above data set is the representative of the individual mouse of BALB/c strain.

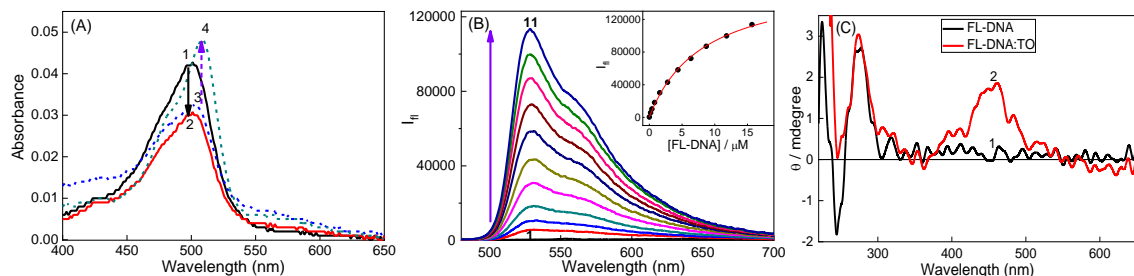


Fig. S12 (A) Absorption of TO with $[FL\text{-DNA}] / \mu\text{M}$: (1) 0, (2) 0.2, (3) 0.4, 4) 16.; (B) Fluorescence of TO with $[FL\text{-DNA}] / \mu\text{M}$, (1) 0, (2) 0.2, (3) 0.4, (4) 0.8, (5) 2, (6) 3, (7) 4, (8) 6, (9) 9, (10) 12, (11) 16; (C) CD spectra of TO with (1) FL-DNA (200 μM), (2) FL-DNA (200 μM):TO (100 μM). Inset in (B) shows the binding isotherm of TO with the FL-DNA. The above data set is the representative of the individual mouse of Swiss albino strain.